

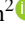




cPro: Circular Projections Using Gradient Descent

Raphael Buchmüller¹ , Bastian Jäckl¹ , Michael Behrisch² , Daniel A. Keim¹ , and Frederik L. Dennig¹ 

¹University of Konstanz, Germany
²Utrecht University, Netherlands

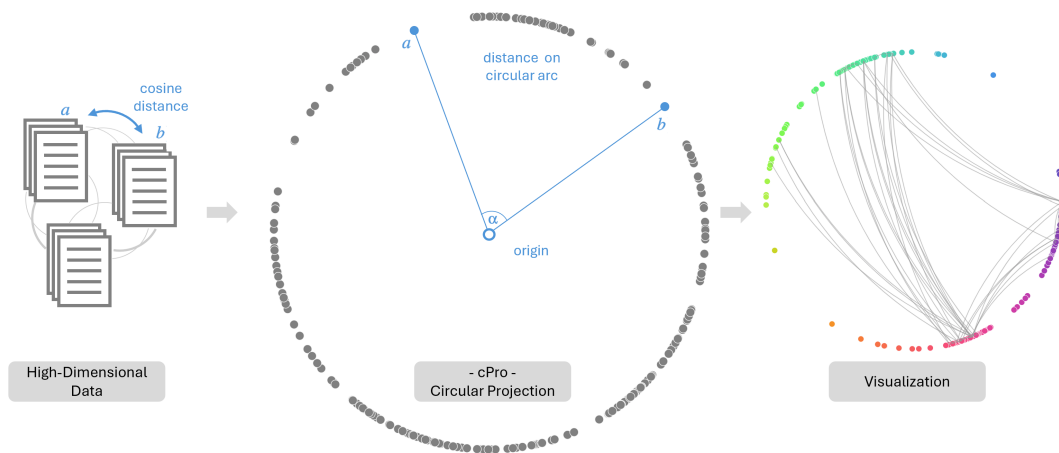


Figure 1: We apply our circular projection technique –cPro– to a high-dimensional text dataset of a collaboration network. Our technique enables the visualization of linked clusters on a circular layout and thus creates a basis for circular visualizations, such as chord diagrams.

Abstract

Typical projection methods such as PCA or MDS rely on mapping data onto an Euclidean space, limiting the design of resulting visualizations to lines, planes, or cubes and thus may fail to capture the intrinsic non-linear relationships within data, resulting in inefficient use of two-dimensional space. We introduce the novel projection technique –cPro–, which aligns high-dimensional data onto a circular layout. We apply gradient descent, an adaptable optimization technique to efficiently reduce a customized loss function. We use selected distance measures to reduce high data dimensionality and reveal patterns on a two-dimensional ring layout. We evaluate our approach compared to 1D and 2D MDS and discuss further use cases and potential extensions. cPro enables the design of novel visualization techniques that employ semantic distances on a circular layout.

CCS Concepts

• **Human-centered computing** → Visualization techniques;

1. Introduction

Visualizing high-dimensional data remains a challenge in the field of data analysis. The complexity and intricacy inherent in such datasets demand advanced methods for effective representation and exploration. Projection methods have emerged as a crucial tool in this context, offering a means to distill high-dimensional information into more comprehensible forms. Typical projection methods, including Principal Component Analysis (PCA) [Jol86] and Multi-dimensional Scaling (MDS) [Kru64], have been instrumental in un-

veiling complex data structures, enabling analysts to perceive patterns and relationships that would otherwise remain hidden in high-dimensional spaces. The concept of cPro originated from identifying a need within the visualization domain to effectively organize items in a ring-like formation based on inherent distances, for which we observed a notable gap in the existing literature.

As evidenced by works in statistics like those by Mardia [Mar72] and Fisher et al. [FLE87], certain types of data, such as directional data, are more effectively described through spherical representa-

tions. This understanding is supported by examples ranging from protein structure [TC02] to observed wind directions. Additionally, in numerous challenges such as text analysis or image classification [DJP06], data frequently undergoes normalization during pre-processing to emphasize its directional distribution. Despite this, only a limited number of machine learning methods actively consider the inherently spherical characteristics of certain types of data during the modeling phase.

Conventional projection methods primarily rely on transforming data from and into Euclidean spaces, usually n -dimensional to two-dimensional planes. This approach, while useful, inherently limits their applicability to a planar topology and bounds the potential of visualization designs. The fundamental geometric limitations of Euclidean spaces — their unbounded and non-compact nature — are incompatible with the properties of a sphere, which is compact, bounded, and closed. This difference raises critical questions: How do classical DR approaches, which assume Euclidean space, fair when projecting data embedded on a spherical manifold? Are we limiting our visualization capabilities by confining ourselves to planar representations? Addressing the mentioned challenges, our contributions are as follows:

- We introduce cPro, the first technique specifically designed to create ring-shaped projections, offering a novel perspective for data visualization.
- Through a detailed comparative evaluation, we illuminate the limitations of traditional planar projection methods when applied to data that inherently aligns better with spherical geometries or cosine distances.
- We explore potential applications of cPro and outline directions for future research to expand the repertoire of visualization designs for novel representation strategies.

2. Related Work

Dimensionality reduction techniques, extensively surveyed in the fields of data analysis and machine learning, aim to simplify complex datasets by lowering their dimensionality [vdM-PvdH09, SVP14, CG15, NA19, EMK*21]. Common methods, such as PCA [Jol86] and MDS [Kru64], and t-distributed Stochastic Neighbor Embedding (t-SNE) [vdMH08], prioritize the preservation of usually Euclidean pairwise distances or local neighborhoods to create projections on planar space.

Extensions aim at addressing data with an intrinsic spherical structure: Circular PCA [Sch07] modifies traditional PCA to include the radial structure of data by constraining the output to a closed curve structure. Persistent Cohomology [dSVJ09] offers a framework to detect and derive circle-valued, low-dimensional representations of manifolds. Hyperspherical Variational Auto-Encoders (VAE) [DFC*22] utilize a von Mises-Fisher distribution. This choice addresses the shortcomings associated with conventional VAEs using Gaussian priors, such as the Origin Gravity Effect in low dimensions and the Soap Bubble Effect in high dimensions, making them better suited for spherical manifolds. Radial projections are also relevant network data: For instance, Circular Graph Embeddings [KT10] map graph data onto a circular spatial embedding suitable for visualization on a sphere.

Radial visualizations, recognized for their compact, space-efficient layouts and visual appeal, have been extensively reviewed

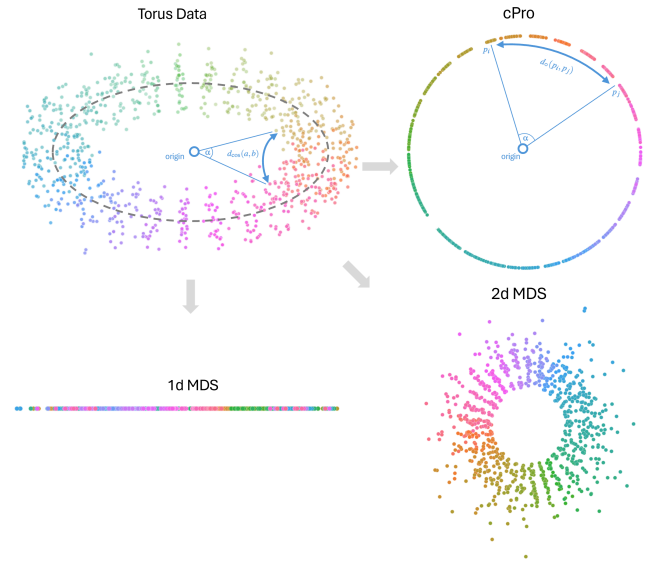


Figure 2: Given a torus dataset, cPro preserves angular relationships and disc-like clusters compared to 2D and 1D MDS.

in the literature [DLR09, DBB10, BW14, WDG*20]. For example, Chord diagrams arrange data points in a circular layout, with arcs linking them to illustrate relationships. Typically, the placement of these data points follows either an inherent order or is allocated for visual clarity [RLBD20, GMB23]. Similar patterns are observed in Radar charts [ALBR16], where quantities are depicted on radial axes emanating from a central point. Star Coordinates and their variants [Kan00, HGM*97, NS11, ZNN16] also employ axis vectors evenly spaced around a center. In contrast to the mentioned techniques, cPro is designed to create spatial arrangements on a circular layout to reflect distances from a high-dimensional data space.

3. cPro: Circular Projection

We begin by defining the notations utilized throughout our work using common notations for projection techniques. Consider a dataset $D := \{x_i\}$, where each sample $x_i \in \mathbb{R}^n$ represents an n -dimensional data point with $1 \leq i \leq |D|$ for $|D|$ samples. The cPro algorithm aims to project such high-dimensional data points onto the one-dimensional circumference of a circle, which we formally describe as $P_o : \mathbb{R}^n \mapsto [0, 1) \subset \mathbb{R}$. Thus, let $P_o(x_i) := p_i$ the projection of x_i on a 1-sphere (i.e., the circumference of a circle) described by an angular value relative to a fixed point on the circumference. Note that, from this value, we can easily compute a two-dimensional coordinate, i.e., $(r \cos(p_i \times 2\pi r), r \sin(p_i \times 2\pi r))$ for the projected point p_i and radius r . Furthermore, let $P := \{P_o(x_i) \mid x_i \in D\}$ the set of all projected points. We further employ Gradient Descent [Ama93] to optimize a loss function $\mathcal{L} : (\mathbb{R}^{|D|} \times |D|, \mathbb{R}^{|D|}) \mapsto \mathbb{R}$. This algorithm iteratively converges to a solution, with k , the number of iterations limiting the maximum execution steps and η defining the learning rate, i.e., the adaptation strength applied in each iteration.

To capture the angular relationships between data points in D , we measure the cosine distance of vectors in high-dimensional space.

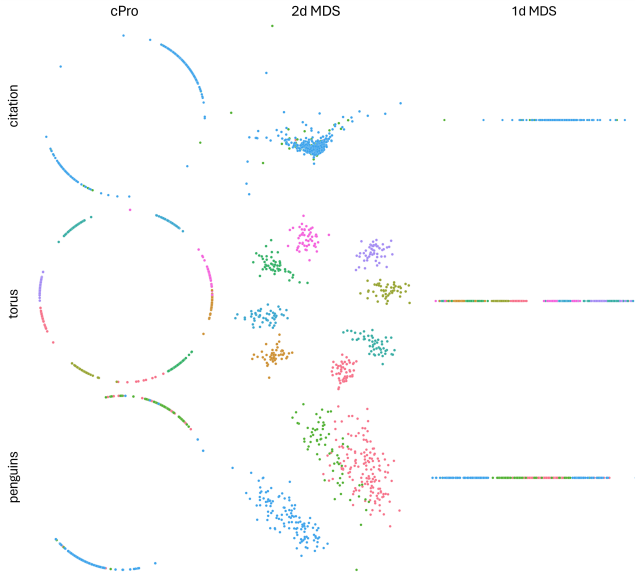


Figure 3: cPro creates circular structures forming groupings on arc sections in contrast to planar projection techniques. We test against 2D and 1D MDS projections on different datasets such as citations, torus, and penguins.

Thus, we define $d_{\cos} : (a, b) \mapsto [0, 1] \subset \mathbb{R}$ with $a, b \in \mathbb{R}^n$ as follows:

$$d_{\cos}(a, b) := \frac{1}{2} \left(1 - \frac{\sum_{i=1}^n a_i \cdot b_i}{\sqrt{\sum_{i=1}^n (a_i)^2} \cdot \sqrt{\sum_{i=1}^n (b_i)^2}} \right) \quad (1)$$

Note that, in this definition, we scale the standard cosine distance to a range of $(0, 1)$, yielding a value of 0 for vectors of the same angle, $\frac{1}{2}$ for orthogonal vectors, and 1 for vectors pointing in the opposite direction. This scaling allows us to omit a scaling inside the loss function, which is repeatedly computed; additionally, it is easier to understand.

On the low-dimensional side, we define the distance on the circumference of a circle $d_o : (a, b) \mapsto [0, 1] \subset \mathbb{R}$ with $a, b \in [0, 1] \subset \mathbb{R}$ describing 1-dimensional positions on the circumference of the circle. Thus, we define this function as:

$$d_o(a, b) := 2 \cdot \min(\|a - b\|, 1 - \|a - b\|) \quad (2)$$

The maximum possible distance is reached if two points are placed directly opposite to each other, i.e., halfway around the circle, expressed as $d_o(a, b) = 1$. Additionally, if $a = 0$ and $b = 1$, these points should be placed at the same location since their relative angle is 0, i.e., b is placed a "full circle" away from a . Thus, we use the minimum function to achieve this circular behavior. We can do this since the length of the arc L on a circle circumference with radius r is geometrically defined as $L = r\alpha$ for angle α in radians. Independent of factor r , we have $\alpha = 2\pi \cdot d_o(a, b)$. The cPro projection technique leverages gradient descent [BV04] a custom loss function \mathcal{L} (see Equation 3) to map high-dimensional cosine distances in D to a lower-dimensional circular space. Inspired by state-of-the-art MDS implementations [dLM09], we de-

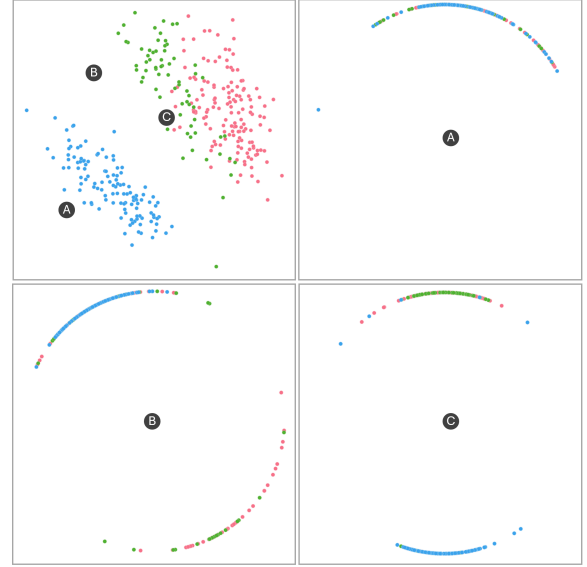


Figure 4: cPro with three different origins (A–C) applied. Selecting an appropriate high-dimensional origin as approximately displayed on the PCA projection (top-left) is crucial. The points B and C separate the clusters more clearly compared to point A.

fine a loss function that measures the *difference* between angular distances through d_{\cos} (see Equation 1) in high-dimensional space and low-dimensional space with d_o (see Equation 2). The high-dimensional angular distances are represented by the distance matrix $M := \{m_{i,j}\}$ with $m_{i,j} = d_{\cos}(x_i, x_j)$ for samples $x_1, \dots, x_{|D|}$. We define all projected points as $P := \{p_1, \dots, p_{|D|}\}$, which are iteratively updated during Gradient Descent. Finally, we define the loss function \mathcal{L} as:

$$\mathcal{L}(M, P) := \frac{1}{|D|^2} \sum_{i=1}^{|D|} \sum_{j=1}^{|D|} |m_{i,j} - d_o(p_i, p_j)| \quad (3)$$

The distance matrix M is fixed during Gradient Descent. We add $\frac{1}{|D|^2}$ as a normalization factor, allowing for a quality comparison between datasets of different sizes. The remainder sums overall differences in high- and low-dimensional distances. One benefit of cPro lies in the projection of spherical or circular-shaped data, which maintains angular relations. By optimizing for this criterion, we make it particularly suitable for datasets with more relevant relationships, such as textual/document similarity or computer vision. The algorithm *runtime* and *steerability* directly depend on the specified parameter set of the gradient descent optimizer. The complete code for projection is added to the supplementary material and will be made publicly available.

Translation: Our approach is dependent on the position of the origin, i.e., the position at which the angle between two vectors is measured, as defined by the cosine distance. Thus, our technique enforces a "relative perspective" on the data as shown in Figure 4. Our preliminary tests show that using the data mean as the gravitational center (Point C) provides the best results while the circumcenter is more likely to create highly dense clusters and misallocations, forcing originally close points towards opposite, radial

Dataset	Metric	cPro			1D MDS			2D MDS		
		Euc.	Cos.	Man.	Euc.	Cos.	Man.	Euc.	Cos.	Man.
Citations	Stress (↓)	.99	.06	.99	.99	1.43	.99	.99	1.08	.99
	Correlation (↑)	.68	1.0	.69	.04	.01	.41	.69	.21	.68
	Silhouette (↑)	-.20	-.25	-.19	-.30	-.25	-.30	-.18	-.29	-.20
	Trustworthiness (↑)	.63	.64	.62	.75	.67	.76	.86	.95	.86
	Avg Dist (↓)	.54	.50	.74	1.38	1.00	1.38	1.59	.90	2.06
Penguins	Stress (↓)	.99	.03	.99	.99	.93	.99	.99	.61	.99
	Correlation (↑)	.68	1.0	.68	.46	.15	.46	.72	.56	.68
	Silhouette (↑)	.15	.15	.15	.18	.11	.18	.42	.61	.41
	Trustworthiness (↑)	.76	.76	.76	.68	.61	.68	.80	.87	.81
	Avg Dist (↓)	1.01	.98	1.13	1.94	.99	1.94	2.47	.99	3.16
Iris	Stress (↓)	.59	.17	.68	.42	.68	.57	.18	.22	.32
	Correlation (↑)	.84	.97	.84	.73	.57	.73	.95	.94	.95
	Silhouette (↑)	.41	.40	.41	.32	.17	.32	.40	.49	.41
	Trustworthiness (↑)	.82	.84	.82	.90	.72	.91	.98	.95	.97
	Avg Dist (↓)	1.10	.96	1.41	2.09	.99	2.09	2.45	.97	3.11

Table 1: Evaluation measures as presented by Espadoto et al. [EMK*21] for the citation, penguins, and iris datasets. cPro generally outperforms 1D and 2D MDS for cosine similarity but shows disadvantages for euclidean and manhattan distance metrics.

directions. Future work will focus on identifying optimal origin coordinates based on the input data.

Rotation: Given an origin, our approach is rotational invariant since the respective angle of two vectors relative to the origin does not change when rotating the dataset around it. With a non-standard rotation, where the data is rotated around an axis or point that is not aligned or identical to the origin, the rotation will change the outcome of our approach because the relative angle of vectors is changed with respect to the origin.

Scale: With a fixed origin, scaling does not impact the result of our approach since scaling only changes the magnitude of the vectors, which does not influence the outcome of the cosine distance calculations. However, a scaling that impacts the components of each vector individually, like a min-max-normalization, will change the relative angle between vectors.

4. Evaluation

We decided to utilize commonly applied and generated datasets for evaluating cPro by varying the numbers of dimensionality d , target classes K , and number of data points n . This includes the *iris*, *penguins* (Figures 3 and 4) and the *breast_cancer* datasets from scikit-learn (scikit-learn.org, visited on 01.02.2024). To test edge case situations, we used eleven synthetic datasets: spherical data formations *2D*-, *3D*-, *4D*-, *5D-sphere* (Figure 3) and *torus* (Figure 2), clustering patterns (*blobs*, *blobs_3d*), and more complex structures *snakes*, *three_circles*, *unbalanced*. We further retrieved *citational* network data specific for testing cosine distances on high-dimensional, linked document data (Figure 1 and 3).

Following Brandes et al. [BP07], we ensured the robustness of our results by averaging metrics across 100 independent runs. As gradient descent depends on its initialization values, we present the averaged measurements of which we observed negligible variance. We chose Multidimensional Scaling (MDS) for our comparison due to its methodological similarity to cPro, both aiming

Dataset	Dimens. (d)	# Classes (K)	# Points (n)
<i>iris</i>	4	3	150
<i>penguins</i>	6	3	345
<i>breast_cancer</i>	30	2	569
<i>nD-Sphere</i>	2,3,4,5	2	100
<i>torus</i>	3	1000	1000
<i>blobs(3D)</i>	2,3	4,4	200,400
<i>cube</i>	3	4	400
<i>snakes</i>	3	1000	1000
<i>three_circles</i>	2	200	200
<i>unbalanced</i>	2	4	100
<i>citational</i>	8	3	400

Table 2: Datasets used in our evaluation.

to preserve intrinsic data relationships within reduced dimensional spaces and utilizing cosine and Euclidean distances for angular and low-dimensional planar metrics respectively. Additionally, we incorporated Manhattan distance [GLS*15] to provide an independent assessment of performances across both methods.

We find that cPro’s performance highly depends on the set learning parameters and origin point as discussed in the previous section. Based on our experiences, we evaluated our approach by using the gravitational center of the dataset as the origin and executed our experiments with 1000 iterations with a learning rate of 0.05.

5. Discussion

Table 1 shows typical evaluation results (see the supplementary material for the complete evaluation). The superior performance of cPro when utilizing the cosine metric can be attributed to its design, which aligns particularly well with data embedded in spherical spaces. Unlike planar projection methods, such as MDS, which inherently assume an Euclidean space and thus excel in it, cPro is optimized for circular layouts. The technique achieves higher correlation, lower stress, and smaller average distances for datasets based on the cosine metric. The strength of cPro in handling spheri-

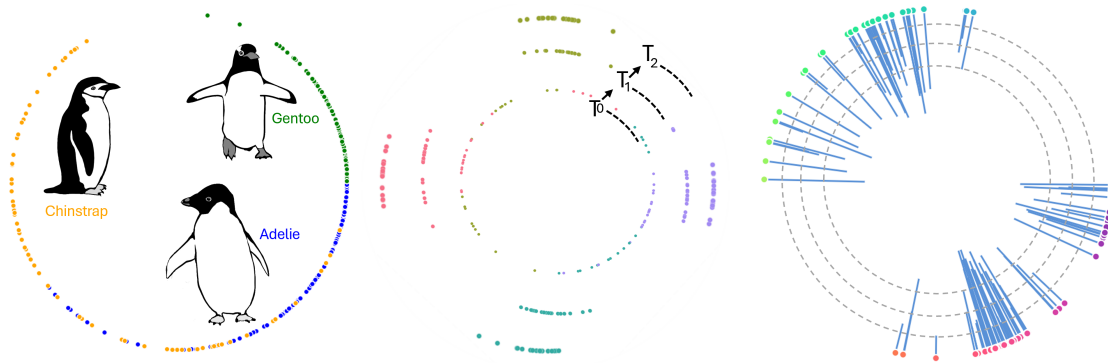


Figure 5: Sketches of future cPro-based designs. cPro allows to utilization of the center space, e.g. to embed a radial inner bar chart (right) and simple legend (left), or designing novel techniques such as introducing temporal attributes through multiple rings (middle).

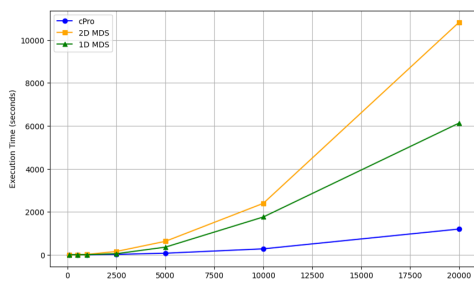


Figure 6: Run time of applied projection techniques by the number of items applied on the snake dataset. We see improvements of cPro being 6.5 and 3.3 times faster compared to 2D and 1D MDS.

cal data also reveals its limitations in terms of Trustworthiness compared to 2D MDS. While cPro can force data points into incorrect groupings due to its radial constraint—evidenced by reduced Trustworthiness scores. Essentially, cPro occupies a unique position between 1D and 2D projections, embodying a trade-off by enhancing Correlation with its circular layout, yet this can affect Trustworthiness as it may condense neighborhoods, distorting original relationships as depicted in Figure 3. Having an additional degree of freedom and thereby enhanced, spatial flexibility, 2D MDS often results in better preservation of neighborhood relations raising the question about the fairness of comparison. Figure 6 illustrates the comparative computational performance of cPro against MDS, evaluated on an AMD Ryzen 7 PRO 5850U 1.90 GHz 8-core processor. The results demonstrate that cPro is approximately 6.5 times and 3.3 times faster than 2D MDS and 1D MDS, respectively.

Other Optimization Strategies: We are aware that the result of Gradient Descent is prone to converge to a local optimum. Thus, we also tested other optimization strategies that are probabilistic and do not make a similar assumption about the loss function. We started designing cPro using Basin-Hopping, which integrates a stochastic global search with a local minimization strategy, making it less likely to get trapped in local optima compared to traditional methods. Secondly, we tested dual annealing [XSFG97] primarily for its proficiency in navigating non-linear response surfaces and its stochastic nature due to its efficacy in handling complex optimization tasks. However, we ultimately chose Gradient Descent for our implementation due to its simplicity and the extensive liter-

ature supporting its effectiveness in various applications despite its potential for local convergence.

Future Work: We believe that cPro has the potential to form the basis for designing novel visualizations as sketched in Figure 5. As visualization designs are often combined with projection techniques to explore high-dimensional data, cPro opens up its center space enabling the display of additional information and data interaction [CMK20]. Future techniques can highlight semantic distances and groupings on the outer ring in combination with selected data attributes as visualized by a barchart (right) or a simple legend (left), or to build upon current projection designs (middle). Similarly, we want to investigate cPro’s potential to extend current visualization designs such as chord diagrams or circular graph layouts. As discussed, cPro is incapable of preserving distances among points at the same angle. We plan to focus on expanding cPro’s performance and applicability, investigating origin positioning and extending spherical projections, as well as investigating alternative optimization strategies to further refine the projection process. We further plan to expand the scope of comparison to include additional projection methods such as PCA.

6. Conclusion

In this paper, we introduced cPro, a novel circular projection technique optimized for high-dimensional data visualization. Utilizing gradient descent, cPro efficiently projects data onto a circular layout, striking a balance between 1D and 2D projections by offering a unique approach to distance representation. While generally underscoring 2D MDS, our evaluation highlights cPro’s efficacy, especially in preserving data relationships prone for cosine distance. While applying well-established evaluation measures [GLS*15] to compare similar projections, we emphasize the need for evaluation measures of spherical dimension reductions. Future directions include broadening cPro’s applications, optimizing origin selection, and refining spherical projections. The potential for cPro to inspire new designs opens an exciting avenue for innovation in the visualization domain.

Acknowledgments – This work was funded by the Federal Ministry of Education and Research (BMBF) in VIKING (13N16242) and by the Deutsche Forschungsgemeinschaft (DFG, German Research Foundation) in RATIO-CUEPAQ (455910360) and TRR 161 (Project A03, 251654672).

References

- [ALBR16] ALBO Y., LANIR J., BAK P., RAFAELI S.: Off the radar: Comparative evaluation of radial visualization solutions for composite indicators. *IEEE Transactions on Visualization and Computer Graphics* 22, 1 (2016), 569–578. doi:10.1109/TVCG.2015.2467322. 2
- [Ama93] AMARI S.-I.: Backpropagation and stochastic gradient descent method. *Neurocomputing* 5, 4 (1993), 185–196. doi:10.1016/0925-2312(93)90006-0. 2
- [BP07] BRANDES U., PICH C.: Eigensolver Methods for Progressive Multidimensional Scaling of Large Data. In *Graph Drawing* (2007), Lecture Notes in Computer Science, Springer, pp. 42–53. doi:10.1007/978-3-540-70904-6_6. 4
- [BV04] BOYD S., VANDENBERGHE L.: *Convex Optimization*. Cambridge University Press, 2004. 3
- [BW14] BURCH M., WEISKOPF D.: On the benefits and drawbacks of radial diagrams. 2014, pp. 429–451. doi:10.1007/978-1-4614-7485-2_17. 2
- [CG15] CUNNINGHAM J. P., GHAHRAMANI Z.: Linear dimensionality reduction: survey, insights, and generalizations. *Journal of Machine Learning Research* 16 (2015), 2859–2900. doi:10.5555/2789272.2912091. 2
- [CMK20] CHATZIMPARMPAS A., MARTINS R. M., KERREN A.: t-viSNE: Interactive assessment and interpretation of t-SNE projections. *IEEE Transactions on Visualization and Computer Graphics* 26, 8 (2020), 2696–2714. doi:10.1109/TVCG.2020.2986996. 5
- [DBB10] DIEHL S., BECK F., BURCH M.: Uncovering strengths and weaknesses of radial visualizations—an empirical approach. *IEEE Transactions on Visualization and Computer Graphics* 16, 6 (2010), 935–942. doi:10.1109/TVCG.2010.209. 2
- [DFC*22] DAVIDSON T. R., FALORSI L., CAO N. D., KIPF T., TOMCZAK J. M.: Hyperspherical variational auto-encoders, 2022. 2
- [DJP06] DIXON M., JACOBS N., PLESS R.: Finding minimal parameterizations of cylindrical image manifolds. In *IEEE Conference on Computer Vision and Pattern Recognition* (2006), IEEE Computer Society, p. 192. doi:10.1109/CVPRW.2006.82. 2
- [dLM09] DE LEEUW J., MAIR P.: Multidimensional scaling using majorization: SMACOF in R. *Journal of Statistical Software* 31, 3 (2009), 1–30. doi:10.18637/jss.v031.i03. 3
- [DLR09] DRAPER G. M., LIVNAT Y., RIESENFELD R. F.: A survey of radial methods for information visualization. *IEEE Transactions on Visualization and Computer Graphics* 15, 5 (2009), 759–776. doi:10.1109/TVCG.2009.23. 2
- [dSVJ09] DE SILVA V., VEJDEMO-JOHANSSON M.: Persistent cohomology and circular coordinates. In *Twenty-Fifth Annual Symposium on Computational Geometry* (2009), Association for Computing Machinery, p. 227–236. doi:10.1145/1542362.1542406. 2
- [EMK*21] ESPADOTO M., MARTINS R. M., KERREN A., HIRATA N. S. T., TELEA A. C.: Toward a Quantitative Survey of Dimension Reduction Techniques. *IEEE Transactions on Visualization and Computer Graphics* 27, 3 (2021), 2153–2173. doi:10.1109/TVCG.2019.2944182. 2, 4
- [FLE87] FISHER N. I., LEWIS T., EMBLETON B. J. J.: *Statistical Analysis of Spherical Data*. Cambridge University Press, 1987. doi:10.1017/CBO9780511623059. 1
- [GLS*15] GREGOR R., LAMPRECHT A., SIPIRAN I., SCHRECK T., BUSTOS B.: Empirical evaluation of dissimilarity measures for 3D object retrieval with application to multi-feature retrieval. In *2015 13th International Workshop on Content-Based Multimedia Indexing* (2015), pp. 1–6. doi:10.1109/CBMI.2015.7153629. 4, 5
- [GMB23] GUTWIN C., MAIRENA A., BANDI V.: Showing flow: Comparing usability of chord and Sankey diagrams. In *CHI Conference on Human Factors in Computing Systems* (2023), Association for Computing Machinery. doi:10.1145/3544548.3581119. 2
- [HGM*97] HOFFMAN P., GRINSTEIN G. G., MARX K. A., GROSSE I., STANLEY E.: DNA visual and analytic data mining. In *8th IEEE Visualization Conference* (1997), IEEE Computer Society and ACM, pp. 437–442. doi:10.1109/VISUAL.1997.663916. 2
- [Jol86] JOLLIFFE I. T.: *Principal Component Analysis*. Springer Series in Statistics. Springer, 1986. doi:10.1007/978-1-4757-1904-8. 1, 2
- [Kan00] KANDOGAN E.: Star coordinates: A multi-dimensional visualization technique with uniform treatment of dimensions. In *IEEE Information Visualization Symposium* (2000). 2
- [Kru64] KRUSKAL J. B.: Multidimensional scaling by optimizing goodness of fit to a nonmetric hypothesis. *Psychometrika* 29 (1964), 1–27. doi:10.1007/BF02289565. 1, 2
- [KT10] KOBATA K., TANAKA T.: A circular embedding of a graph in euclidean 3-space. *Topology and its Applications* 157, 1 (2010), 213–219. doi:10.1016/j.topol.2009.04.055. 2
- [Mar72] MARDIA K. V.: *Statistics of Directional Data*. Probability and Mathematical Statistics: A Series of Monographs and Textbooks. Academic Press, 1972. 1
- [NA19] NONATO L. G., AUPETIT M.: Multidimensional projection for visual analytics: Linking techniques with distortions, tasks, and layout enrichment. *IEEE Transactions on Visualization and Computer Graphics* 25, 8 (2019), 2650–2673. doi:10.1109/TVCG.2018.2846735. 2
- [NS11] NOVÁKOVÁ L., STEPÁNKOVÁ O.: Visualization of trends using RadViz. *Journal of Intelligent Information Systems* 37, 3 (2011), 355–369. doi:10.1007/S10844-011-0157-4. 2
- [RLBD20] REES D., LARAMEE R. S., BROOKES P., D’CRUZE T.: Interaction techniques for chord diagrams. In *24th International Conference Information Visualisation* (2020), pp. 28–37. doi:10.1109/IV51561.2020.00015. 2
- [Sch07] SCHOLZ M.: Analysing periodic phenomena by circular PCA. In *Bioinformatics Research and Development* (2007), vol. 4414 of *Lecture Notes in Computer Science*, Springer, pp. 38–47. doi:10.1007/978-3-540-71233-6_4. 2
- [SVP14] SORZANO C. O. S., VARGAS J., PASCUAL-MONTANO A. D.: A survey of dimensionality reduction techniques. *CoRR abs/1403.2877* (2014). arXiv:1403.2877. 2
- [TC02] TRABI M., CRAIK D. J.: Circular proteins — no end in sight. *Trends in Biochemical Sciences* 27, 3 (2002), 132–138. doi:10.1016/S0968-0004(02)02057-1. 2
- [vdMH08] VAN DER MAATEN L., HINTON G.: Visualizing data using t-SNE. *Journal of Machine Learning Research* 9, 86 (2008), 2579–2605. URL: <http://jmlr.org/papers/v9/vandermaaten08a.html>. 2
- [vdMPvdH09] VAN DER MAATEN L., POSTMA E., VAN DEN HERIK J.: *Dimensionality Reduction: A Comparative Review*. Tech. Rep. TiCC TR 2009-005, Tilburg University, Netherlands, 2009. 2
- [WDG*20] WALDNER M., DIEHL A., GRAČANIN D., SPLECHTNA R., DELRIEUX C., MATKOVIĆ K.: A comparison of radial and linear charts for visualizing daily patterns. *IEEE Transactions on Visualization and Computer Graphics* 26, 1 (2020), 1033–1042. doi:10.1109/TVCG.2019.2934784. 2
- [XSFG97] XIANG Y., SUN D. Y., FAN W., GONG X. G.: Generalized simulated annealing algorithm and its application to the Thomson model. *Physics Letters A* 233, 3 (1997), 216–220. doi:10.1016/S0375-9601(97)00474-X. 5
- [ZNN16] ZANABRIA G. G., NONATO L. G., NIETO E. G.: iStar (i*): An interactive star coordinates approach for high-dimensional data exploration. *Computer Graphics* 60 (2016), 107–118. doi:10.1016/J.CAG.2016.08.007. 2